



Variation of Coster-Kronig enhancement factors at different excitation energies of the elements in the atomic number range $41 \leq Z \leq 49$

Rafet YILMAZ^{1,*}, Turgay ÖZMEN², Tahir ÇAKIR³

on the last page

¹Department of Physics, Faculty of Science, Yuzuncu Yil University 65080, Van, Turkey,

²Institute of Sciences, Yuzuncu Yil University, 65080, Van, Turkey..

³Department of Biophysics, Faculty of Medical, Yuzuncu Yil University, 65080, Van, Turkey

Received: 17 October 2019; Revised: 11 November 2019; Accepted: 13 November 2019

*Corresponding author e-mail: ryilmaz@yyu.edu.tr

Citation: Yılmaz, R.; Özmen, T.; Çakır, T. *Int. J. Chem. Technol.* 2019, 3 (2), 101-112.

ABSTRACT

In this study, L X-ray fluorescence (XRF) cross-sections of elements with atomic number $41 \leq Z \leq 49$ were theoretically calculated according to different excitation energies. Also, the Coster-Kronig (CK) enhancement factors observed as a result of the effect of non-irradiated Coster-Kronig transitions on L X-ray fluorescence cross-sections were theoretically calculated at different excitation energies. The change of both L XRF fluorescence cross-sections and the Coster-Kronig enhancement factors against energy were examined. The results obtained were compared with the values in the literature.

Keywords: X-ray fluorescence cross-sections, Coster-Kronig enhancement factors, cross-sections.

Atom numarası $41 \leq Z \leq 49$ arasındaki elementlerin farklı uyarma enerjilerinde Coster-Kronig şiddetlendirme faktörlerinin değişimi

ÖZ

Bu çalışmada, atom numarası $41 \leq Z \leq 49$ arasındaki elementlerin L X-ışını floresans tesir kesitleri, farklı uyarma enerjilerine göre teorik olarak hesaplanmıştır. Ayrıca, ışımaz Coster-Kronig geçişlerinin L X ışını floresans tesir kesitleri üzerindeki etkisinin sonucu olarak gözlenen Coster-Kronig şiddetlendirme faktörleri, farklı uyarma enerjilerinde teorik olarak hesaplandı. Hem L X- ışını floresans kesitlerinin hem de Coster-Kronig şiddetlendirme faktörlerinin enerjiye karşı değişimi incelendi. Elde edilen sonuçlar literatürdeki değerler ile mukayese edildi.

Anahtar Kelimeler: X-ışını floresans tesir kesitleri, Coster-Kronig şiddetlendirme faktörleri, tesir kesitleri.

1. INTRODUCTION

X-ray fluorescence (XRF) cross-sections are of great importance with the extensive use in the fields of molecular, atomic, and radiation physics. Besides, in photon-matter mutual effects of some materials, XRF cross-sections have wide research fields. Especially, the usage of some substances in the field of medicine increases the importance of this work.

XRF cross-sections are identified as the result of photoelectric cross-sections and fluorescence yields at appropriate excitation energy. However, in the case of the

L shell, particularly the L_3 subshell X-ray lines, the estimation of XRF cross-sections is not so straight forward because of the possibility of Coster-Kronig (CK) transitions. These transitions are non-radiative transitions. These transitions from L_1 and L_2 to L_3 lead to an additional gap in the L_3 subshell. The number of X-rays is generated as a result of this increases.¹ Rani and co-workers have reported the effect of CK enhancement factor on the XRF cross-sections.² There are many researchers who have examined XRF cross-sections, CK transitions; fluorescence yields for some elements.³⁻¹³

In recent years, Kumar and co-workers have investigated the Sm element at different energies of 6.8, 7.4 and 8 keV.¹⁴ Öz and co-workers did the same work for some elements in between $Z = 66$ and $Z = 90$.^{15,16} Previously, we have also done experimental and theoretical studies on this topic for Yb, Lu, Os and Pt.¹⁷

This study presents originality because of the investigation of the change of XRF cross sections and CK enhancement factors at different excitation energies of same elements in the atomic number range $41 \leq Z \leq 49$. Herein, firstly, L-XRF cross-sections have been calculated. Secondly, theoretical enhancement factors have been calculated from the obtained values. Excitation energies have been chosen according to the binding energies of electrons.

2. THEORETICAL CALCULATIONS

In this study, the L XRF cross-sections are calculated from the following equations.¹⁵

$$\sigma_{L\ell} = [\sigma_1(f_{13} + f_{12}f_{23}) + \sigma_2f_{23} + \sigma_3]\omega_3F_{3\ell} \quad (1)$$

$$\sigma_{L\alpha} = [\sigma_1(f_{13} + f_{12}f_{23}) + \sigma_2f_{23} + \sigma_3]\omega_3F_{3\alpha} \quad (2)$$

$$\sigma_{L\beta} = \sigma_1\omega_1F_{1\beta} + (\sigma_1f_{12} + \sigma_2)\omega_2F_{2\beta} + [\sigma_3 + \sigma_2f_{23} + \sigma_1(f_{13} + f_{12}f_{23})]\omega_3F_{3\beta} \quad (3)$$

Where, σ_1, σ_2 and σ_3 are photo ionization cross-sections determined from the work of Scofield¹⁹ at proper energies. ω_1, ω_2 and ω_3 are fluorescence yields of subshell. f_{12}, f_{13} and f_{23} are the CK transition probabilities. Fluorescence yield and CK transition probabilities were obtained from the work of Krause.²¹ F_{ij} ($F_{3\alpha}, F_{3\ell}, F_{3\beta}, F_{2\beta}, F_{1\beta}$) are the fractions of the radiation width of the subshell L_i ($i = 1, 2$ and 3). The F_{ij} values are given in Table 1.

$$F_{ij} = \frac{\Gamma_{ij}}{\Gamma} \quad \text{e.g.} \quad F_{3\ell} = \frac{\Gamma_{3\ell}}{\Gamma} \quad (4)$$

Where, Γ is theoretically the total radiative transition rate of the L_3 . $\Gamma_{3\alpha}$ is the sum of the radiative transition rates associated with filling the gaps in the L_3 shell. That is;

$$\Gamma_{3\ell} = \Gamma_3(M_1 - L_3) \quad (5)$$

$$\Gamma_{3\alpha} = \Gamma_3(M_4 - L_3) + \Gamma_3(M_5 - L_3) \quad (6)$$

$$\Gamma_{3\beta} = \Gamma_3(N_1 - L_3) + \Gamma_3(N_4 - L_3) + \Gamma_4(N_5 - L_3) + \Gamma_3(O_1 - L_3) + \Gamma_3(O_4, O_5 - L_3) \quad (7)$$

$$\Gamma_{2\beta} = \Gamma_2(M_4 - L_2) + \Gamma_2(M_3 - L_2) \quad (8)$$

$$\Gamma_{1\beta} = \Gamma_1(M_2, M_3 - L_1) + \Gamma_1(M_4, M_5 - L_1) \quad (9)$$

Scofield calculated the radiative transition rates - Slater theory for most elements.^{18,20} In the absence of the CK transitions, the cross sections can be calculated from the following equations.¹⁵

$$\sigma_{L\ell} = \sigma_3\omega_3F_{3\ell} \quad (10)$$

$$\sigma_{L\alpha} = \sigma_3\omega_3F_{3\alpha} \quad (11)$$

$$\sigma_{L\beta} = \sigma_1\omega_1F_{1\beta} + \sigma_2\omega_2F_{2\beta} + \sigma_3\omega_3F_{3\beta} \quad (12)$$

Because the CK transitions exist, L XRF were evaluated according to Equations 1-3. The CK enhancement factors κ_{ij} ($i = \ell, \alpha; j = 1, 2$) can be calculated from the following equations.^{15,16}

$$\kappa_{(i,j)} = \frac{\sigma_1(f_{13} + f_{12}f_{23}) + \sigma_2f_{23} + \sigma_3}{\sigma_3} \quad (13)$$

$$\kappa_{\beta} = \frac{\sigma_1\omega_1F_{1\beta} + (\sigma_1f_{12} + \sigma_2)\omega_2F_{2\beta}}{\sigma_1\omega_1F_{1\beta} + \sigma_2\omega_2F_{2\beta} + \sigma_3\omega_3F_{3\beta}} \quad (14)$$

$$+ \frac{[\sigma_3 + \sigma_2f_{23} + \sigma_1(f_{13} + f_{12}f_{23})]\omega_3F_{3\beta}}{\sigma_1\omega_1F_{1\beta} + \sigma_2\omega_2F_{2\beta} + \sigma_3\omega_3F_{3\beta}}$$

In this study, the theoretical values of L XRF cross-sections (Table 2-5), and enhancement factors (Tables 9 and 10) were calculated for close excitation energy to absorption edge energy of the studied elements. Also, the theoretical values of L XRF cross-sections (Table 6-8), and enhancement factors (Tables 11 and 12) were calculated for the greater excitation energy from the absorption edge energy of the same elements.

3. RESULTS AND DISCUSSION

The L subshell X-ray fluorescence cross-sections have been calculated from Equations (1-3) for close excitation energy to absorption edge energy and the greater from the absorption edge energy of studied elements (Table 2-8). The enhancement factors have been calculated theoretically from Equations (13) and (14), and listed in Tables 9-12.

Table 1. Theoretically calculated fractions of the radiation width

Element	Fraction of radiative widths				
	$F_{3\ell}$	$F_{3\alpha}$	$F_{1\beta}$	$F_{2\beta}$	$F_{3\beta}$
⁴¹ Nb	0.035	0.934	0.862	0.941	0.028
⁴² Mo	0.035	0.926	0.857	0.877	0.029
⁴³ Tc	0.034	0.918	0.853	0.924	0.044
⁴⁴ Ru	0.034	0.918	0.850	0.914	0.056
⁴⁵ Rh	0.033	0.899	0.847	0.905	0.066
⁴⁶ Pd	0.033	0.888	0.845	0.893	0.078
⁴⁷ Ag	0.032	0.880	0.841	0.885	0.087
⁴⁸ Cd	0.032	0.871	0.837	0.877	0.094
⁴⁹ In	0.032	0.865	0.832	0.839	0.101

Table 2. L_3 XRF cross-sections (barns/atom) for $41 \leq Z \leq 49$

Element	E (keV)	$\sigma_{L\alpha}$	$\sigma_{L\beta}$	$\sigma_{L\ell}$
⁴¹ Nb	2.386	7625.568	228.603	285.754
⁴² Mo	2.539	7631.860	239.010	288.461
⁴³ Tc	2.696	7594.797	364.020	281.288
⁴⁴ Ru	2.858	7592.429	463.154	281.201
⁴⁵ Rh	3.025	7406.914	543.777	271.888
⁴⁶ Pd	3.193	7179.044	630.591	266.788
⁴⁷ Ag	3.373	7143.136	706.196	252.413
⁴⁸ Cd	3.560	7152.512	769.280	269.992
⁴⁹ In	3.754	6961.347	812.827	257.528

Table 3. L_3 XRF cross-sections (barns/atom) according to the excitation energies of L_2 and L_1 for $41 \leq Z \leq 49$ (for close excitation energy to absorption edge energy)

Element	E(keV)	$\sigma_{L\alpha}$	$\sigma_{L\beta}$	σ_{L1}
^{41}Nb	2.674	5697.343	2839.378	213.497
	3.000	4188.616	2456.635	157.044
^{42}Mo	2.648	6744.817	3342.646	254.933
	3.000	5020.601	2827.232	187.736
^{43}Tc	2.818	6700.373	3683.536	248.159
	4.000	2640.682	1716.435	097.803
^{44}Ru	2.993	6690.843	3747.400	247.911
	4.000	3113.195	2058.982	115.303
^{45}Rh	3.174	6526.900	3714.000	239.585
	4.000	3570.090	2428.620	131.048
^{46}Pd	3.356	6429.333	3843.551	238.830
	4.000	4100.701	2888.952	152.389
^{47}Ag	3.553	6292.457	3954.592	222.353
	4.000	4683.993	3396.644	165.516
^{48}Cd	3.757	6966.109	4052.371	236.747
	4.022	5295.610	3918.681	200.637
^{49}In	3.970	6194.265	3941.396	229.152
	4.244	5265.774	3925.979	194.688

Table 4. L_2 XRF cross-sections (barns/atom) for $41 \leq Z \leq 49$ (for close excitation energy to absorption edge energy)

Element	E(keV)	$\sigma_{L\alpha}$	$\sigma_{L\beta}$	σ_{L1}
^{41}Nb	2.674	6108.629	2851.708	228.886
^{42}Mo	2.648	7257.042	3388.869	274.294
^{43}Tc	2.818	7220.373	3708.668	267.266
^{44}Ru	2.993	7224.441	3779.950	267.495
^{45}Rh	3.174	7053.793	3822.853	258.752
^{46}Pd	3.356	6942.178	3885.831	257.212
^{47}Ag	3.553	6809.397	4005.698	281.943
^{48}Cd	3.757	6768.870	4108.506	256.397
^{49}In	3.970	6706.630	4241.221	248.106

Table 5. L_I XRF cross-sections (barns/atom) for $41 \leq Z \leq 49$ (for close excitation energy to absorption edge energy)

Element	E(keV)	$\sigma_{L\alpha}$	$\sigma_{L\beta}$	σ_{L_I}
⁴¹ Nb	3.000	5316.673	2607.498	199.289
⁴² Mo	3.000	6244.808	3021.255	233.355
⁴³ Tc	4.000	6223.393	3708.668	128.708
⁴⁴ Ru	4.000	4070.968	2222.024	150.701
⁴⁵ Rh	4.000	4620.362	2621.057	169.577
⁴⁶ Pd	4.000	5260.494	3117.180	195.211
⁴⁷ Ag	4.000	5940.055	3662.148	179.088
⁴⁸ Cd	4.022	6659.311	4060.067	252.200
⁴⁹ In	4.244	6653.893	4001.221	246.155

Table 6. L_3 XRF cross-sections (barns/atom) according to the excitation energies of L_2 and L_I for $41 \leq Z \leq 49$ (for the greater excitation energy from the absorption edge energy)

Element	E(keV)	$\sigma_{L\alpha}$	$\sigma_{L\beta}$	σ_{L_I}
⁴¹ Nb	2.695	5583.339	2787.361	209.225
	4.000	1894.626	1164.554	070.997
⁴² Mo	2.844	5706.678	2796.619	215.695
	4.000	2252.623	1273.443	085.142
⁴³ Tc	3.000	5782.665	3126.733	214.172
	5.000	1408.542	0965.655	052.168
⁴⁴ Ru	3.201	5708.729	3156.636	211.434
	5.000	1663.671	1152.588	061.617
⁴⁵ Rh	3.388	5586.511	3211.117	205.066
	5.000	1913.325	1359.586	070.233
⁴⁶ Pd	3.605	5408.541	3392.380	201.222
	5.000	2200.314	1613.727	081.768
⁴⁷ Ag	3.780	5422.560	3407.000	197.184
	5.000	2511.400	1921.502	091.270
⁴⁸ Cd	4.000	5370.237	3493.566	203.464
	5.000	2919.386	2264.099	110.600
⁴⁹ In	4.000	6082.060	3991.672	225.004
	6.000	2019.948	1639.340	074.726

Table 7. L_2 XRF cross-sections (barns/atom) for $41 \leq Z \leq 49$ (for the greater excitation energy from the absorption edge energy)

Element	E(keV)	$\sigma_{L\alpha}$	$\sigma_{L\beta}$	σ_{Ll}
⁴¹ Nb	2.695	5887.238	2799.469	224.289
⁴² Mo	2.844	6130.816	2809.902	232.519
⁴³ Tc	3.000	6223.393	3147.858	230.449
⁴⁴ Ru	3.201	6157.500	3184.012	228.137
⁴⁵ Rh	3.388	6032.992	3243.895	221.266
⁴⁶ Pd	3.605	5846.604	3430.553	217.010
⁴⁷ Ag	3.780	5867.911	3451.123	213.353
⁴⁸ Cd	4.000	5818.940	3542.788	220.351
⁴⁹ In	4.000	6598.061	4040.626	244.262

Table 8. L_l XRF cross-sections (barns/atom) for $41 \leq Z \leq 49$ (for the greater excitation energy from the absorption edge energy)

Element	E(keV)	$\sigma_{L\alpha}$	$\sigma_{L\beta}$	σ_{Ll}
⁴¹ Nb	4.000	2533.348	1268.200	094.924
⁴² Mo	4.000	2985.482	1384.233	112.813
⁴³ Tc	5.000	1942.690	1054.580	071.940
⁴⁴ Ru	5.000	2273.575	1259.831	084.169
⁴⁵ Rh	5.000	2579.149	1485.808	094.604
⁴⁶ Pd	5.000	2940.096	1766.050	104.826
⁴⁷ Ag	5.000	3325.721	2098.281	120.842
⁴⁸ Cd	5.000	3838.101	2453.548	145.329
⁴⁹ In	6.000	2726.847	1813.878	100.877

Table 9. $\kappa_{l1} - \kappa_{\alpha 1}$; $\kappa_{l2} - \kappa_{\alpha 2}$ CK enhancement factors for $41 \leq Z \leq 49$ (for close excitation energy to absorption edge energy)

Element	E(keV) (for L ₂)	$\kappa_{\alpha 1} - \kappa_{l1}$	E(keV) (for L ₁)	$\kappa_{\alpha 2} - \kappa_{l2}$
⁴¹ Nb	2.674	1.072	3.000	1.269
⁴² Mo	2.648	1.075	3.000	1.243
⁴³ Tc	2.818	1.077	4.000	1.316
⁴⁴ Ru	2.993	1.079	4.000	1.307
⁴⁵ Rh	3.174	1.080	4.000	1.294
⁴⁶ Pd	3.356	1.079	4.000	1.282
⁴⁷ Ag	3.553	1.082	4.000	1.268
⁴⁸ Cd	3.757	1.083	4.022	1.257
⁴⁹ In	3.970	1.082	4.244	1.263

Table 10. $\kappa_{\beta 1}$, $\kappa_{\beta 2}$ CK enhancement factors for $41 \leq Z \leq 49$ (for close excitation energy to absorption edge energy)

Element	E(keV) (for L ₂)	$\kappa_{\beta 1}$	E(keV) (for L ₁)	$\kappa_{\beta 2}$
⁴¹ Nb	2.674	1.004	3.000	1.061
⁴² Mo	2.648	1.013	3.000	1.068
⁴³ Tc	2.818	1.007	4.000	1.080
⁴⁴ Ru	2.993	1.008	4.000	1.081
⁴⁵ Rh	3.174	1.020	4.000	1.079
⁴⁶ Pd	3.356	1.011	4.000	1.079
⁴⁷ Ag	3.553	1.012	4.000	1.078
⁴⁸ Cd	3.757	1.013	4.022	1.076
⁴⁹ In	3.970	1.019	4.244	1.076

Table 11. $\mathcal{K}_{l1} - \mathcal{K}_{\alpha 1}$; $\mathcal{K}_{l2} - \mathcal{K}_{\alpha 2}$ CK enhancement factors for $41 \leq Z \leq 49$ (for the greater excitation energy from the absorption edge energy)

Element	E(keV) (for L ₂)	$\mathcal{K}_{\alpha 1} - \mathcal{K}_{l1}$	E(keV) (for L ₁)	$\mathcal{K}_{\alpha 2} - \mathcal{K}_{l2}$
⁴¹ Nb	2.695	1.072	4.000	1.337
⁴² Mo	2.844	1.078	4.000	1.325
⁴³ Tc	3.000	1.076	5.000	1.379
⁴⁴ Ru	3.201	1.079	5.000	1.366
⁴⁵ Rh	3.388	1.079	5.000	1.347
⁴⁶ Pd	3.605	1.080	5.000	1.336
⁴⁷ Ag	3.780	1.082	5.000	1.324
⁴⁸ Cd	4.000	1.083	5.000	1.314
⁴⁹ In	4.000	1.085	6.000	1.349

Table 12. $\mathcal{K}_{\beta 1}$, $\mathcal{K}_{\beta 2}$ CK enhancement factors for $41 \leq Z \leq 49$ (for the greater excitation energy from the absorption edge energy)

Element	E(keV) (for L ₂)	$\mathcal{K}_{\beta 1}$	E(keV) (for L ₁)	$\mathcal{K}_{\beta 2}$
⁴¹ Nb	2.695	1.004	4.000	1.132
⁴² Mo	2.844	1.005	4.000	1.087
⁴³ Tc	3.000	1.006	5.000	1.091
⁴⁴ Ru	3.201	1.008	5.000	1.093
⁴⁵ Rh	3.388	1.010	5.000	1.092
⁴⁶ Pd	3.605	1.011	5.000	1.094
⁴⁷ Ag	3.780	1.012	5.000	1.092
⁴⁸ Cd	4.000	1.014	5.000	1.084
⁴⁹ In	4.000	1.012	6.000	1.106

The graphs of enhancing factors versus atomic number are shown in Figures 1-4. In this study, the results were theoretically until 8.3% for $\mathcal{K}_{\alpha 1}$, until 31.6% for $\mathcal{K}_{\alpha 2}$,

until 8.3% for \mathcal{K}_{l1} , until 31.6% for \mathcal{K}_{l2} , until 1.9% for $\mathcal{K}_{\beta 1}$, until 8% for $\mathcal{K}_{\beta 2}$, for close excitation energy to absorption edge energy.

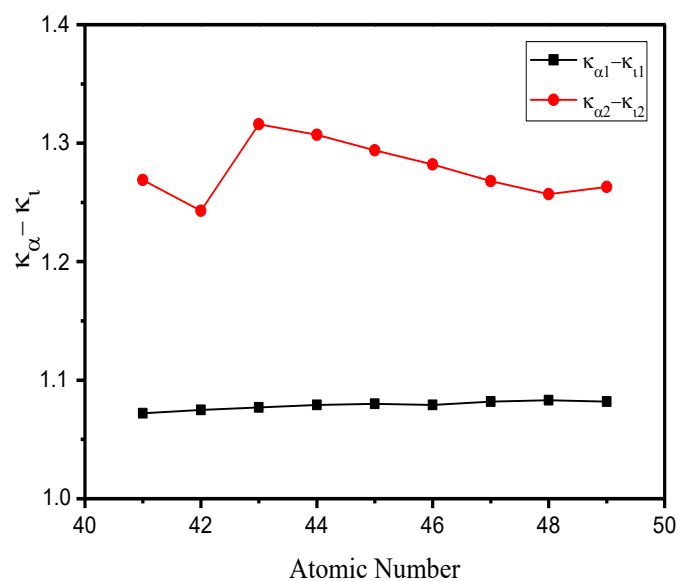


Figure 1. $K_{\alpha 1}$, $K_{\alpha 2}$, K_{l1} , K_{l2} versus atomic number (for close excitation energy to absorption edge energy).

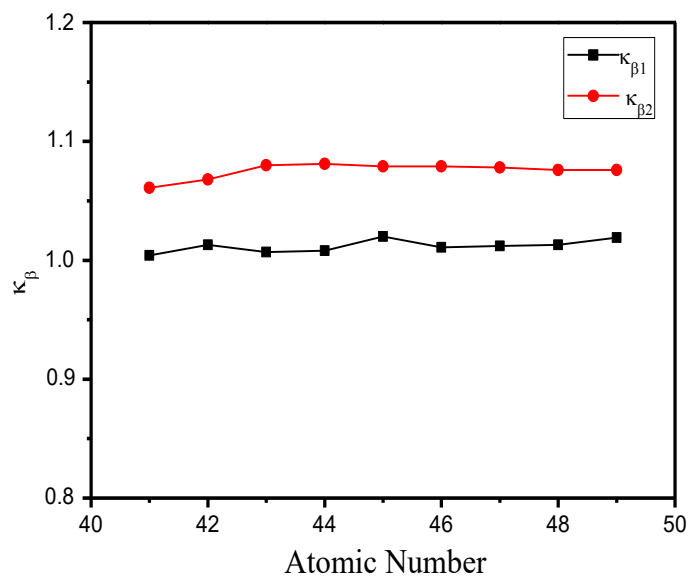


Figure 2. $K_{\beta 1}$, $K_{\beta 2}$ versus atomic number (for close excitation energy to absorption edge energy)

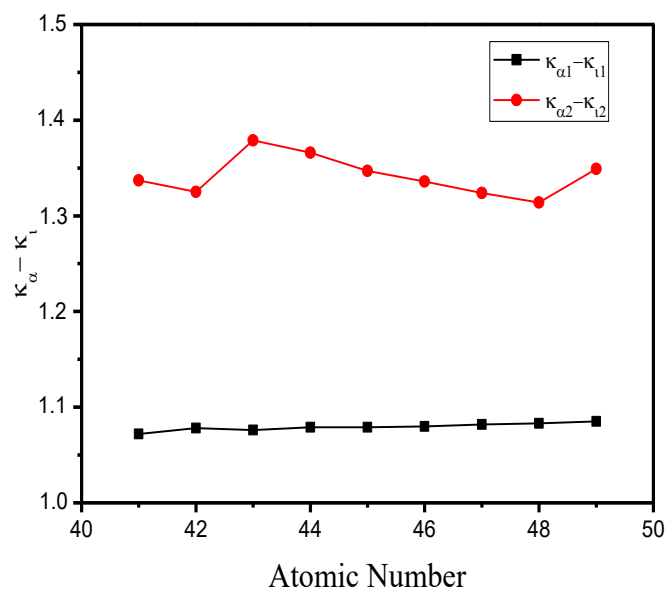


Figure 3. $K_{\alpha 1}$, $K_{\alpha 2}$, $K_{l 1}$, $K_{l 2}$ versus atomic number (for the greater excitation energy from the absorption edge energy).

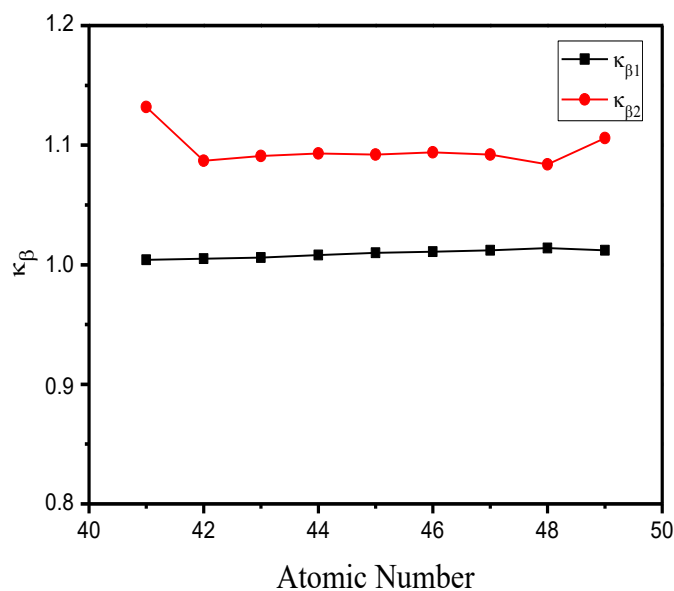


Figure 4. $K_{\beta 1}$, $K_{\beta 2}$ versus atomic number (for the greater excitation energy from the absorption edge energy).

Also, for the greater excitation energy from the absorption edge energy, in the present work, the results were theoretically until 8.5% for $\kappa_{\alpha 1}$, 37.9% for $\kappa_{\alpha 2}$ up to 8.5% for of $\kappa_{\ell 1}$ and up to 37.9% for $\kappa_{\ell 2}$, until 1.4% for $\kappa_{\beta 1}$, until 10.6% for $\kappa_{\beta 2}$.

As seen above, both *L* XRF cross-sections and CK enhancement factor values have been found to vary according to different excitation energies. *L* XRF cross-section values decrease, for the greater excitation energy from the absorption edge energy. However, CK enhancement factors increase. This means that it has increased due to gaps caused by CK transitions. In general, *L* X-ray cross-section values were found to be more efficient in close excitation energy the absorption side.

Rani and co-workers² reported that the effect of on X-ray cross-sections and the CK transitions is up to 65%, experimentally up to 24% for Sb element, theoretically up to 21%. Öz and co-workers reported theoretically up to 30%, experimentally up to 24% for some elements in the atomic number range 66-90.^{15,16}

As can be seen from this study, due to CK transitions, there is an enhancement up to 2-38%. Also, it appears that the X-ray fluorescence cross-sections decrease despite increasing CK enhancement factors for the greater excitation energy from the absorption edge energy. Therefore, the compatibility of the excitation energy and the binding energy is important for efficiency. Thus, it must be taken into account in quantitative X-ray fluorescence cross-sections.

4. CONCLUSIONS

In the present study, the CK enhancement factors due to the effect of CK transitions on *L* XRF cross sections are studied theoretically at different excitation energies. The results of the study can be summarized as follows.

- When the excitation energy is greater than the bonding energy of the electron, XRF cross-sections values decrease, but CK enhancement factors increase.
- When the excitation energy is close to bonding energy of the electron, CK enhancement factors increase but, XRF cross-sections values decrease.

Conflict of interest

Author declares that there is no a conflict of interest with any person, institute, company, etc.

REFERENCES

1. Labar, J. L. *X-ray Spectrom.* **1991**, 20, 111-117.
2. Rani, A.; Nath, N.; Chaturvedi, S. N. *X-ray Spectrom.* **1989**, 18, 77-80.
3. Ertuğrul, M. *J. Elect. Spectrosc. Relat. Phenom.* **2002a**, 125, 69-73.
4. Ertuğrul, M. *Appl. Radiat. Isot.* **2002b**, 57, 63-66.
5. Ertuğrul, M. *J. Quant. Spectrosc. Radiat. Transfer.* **2002c**, 72, 567-574.
6. Tıraşoğlu, E.; Çevik, U.; Ertuğrul, B.; Atalay, Y.; Kopya, A.İ. *Rad. Phys. and Chem.* **2001**, 60 (1-2), 11-16.
7. Han, I; Demir, L.; Ağbaba, M. *Radiat. Phys. And Chem.* **2007**, 76, 1551-1559.
8. Kaya, A.; Ertuğrul, M.; Doğan, O.; Söğüt, Ö.; Turgut, Ü.; Şimşek, Ö. *Anal. Chemica Acta*, **2001**, 441, 317-323.
9. Öz, E.; Özdemir, Y.; Ekinçi, N.; Ertuğrul, M.; Şahin, Y.; Erdoğan, H. *Spec. Acta B*, **2000**, 55, 1869-1877.
10. Öz, E.; Ekinçi, N.; Özdemir, Y.; Ertuğrul, M.; Şahin, Y.; Erdoğan, H. *J. Phys. B: At. Mol. Opt. Phys.* **2001**, 34, 631-638.
11. Puri, S.; Singh, N. *Radiat. Phys. Chem.* **2006**, 75, 2232-2238.
12. Söğüt, Ö.; Büyükkasap, E.; Ertuğrul, M.; Küçükönder, A. *J. Quant. Spectros. Radiat. Trans.* **2002**, 74, 395-400.
13. Hallak, A. B. *Radiat. Phys. Chem.* **2001**, 60, 17-21.
14. Kumar, R.; Rani A.; Singh, R. M.; Tivari M. K.; Singh, A. K., *J. Elect. Spectrosc. Rel. Phen.* **2016**, 209, 34-39.
15. Öz, E.; Ekinçi, N.; Ertuğrul, M.; Şahin, Y. *X-ray Spectrom.* **2003**, 32, 153-157.
16. Öz, E.; Şahin, Y.; Ertuğrul, M.; *Radiat. Phys. Chem.* **2004**, 69, 17-21.
17. Yılmaz, R; Öz, E.; Tan, M.; Durak, R.; Demirel, A. İ.; Şahin, Y. *Radiat. Phys. Chem.* **2009**, 78, 318-322.

DOI: <http://dx.doi.org/10.32571/ijct.634210>

E-ISSN:2602-277X

18. Scofield, J. H. *Phys. Rev. A*, **1969**, 179, 9-16.
19. Scofield, J.H. *Report UCRL Report 51326. Lawrence Livermore Laboratory Report, California*, 1973.
20. Scofield, J. H. *Atom. Data Nucl. Data Tables*. **1974**, 14, 121-137.
21. Krause, M. O. *J. Phys. Chem. Ref. Data*. **1979**, 8, 307-327.

ORCID

 <https://orcid.org/0000-0003-2734-8763> (R. Yılmaz)

 <https://orcid.org/0000-0002-4302-6898> (T. Özmen)

 <https://orcid.org/0000-0003-0080-6605> (T. Çakır)